# Probing the Vulnerability of Large Language Models to Polysemantic Interventions

**Bofan Gong**[*]
Independent Scholar

**Shiyang Lai**[*]
University of Chicago

**Dawn Song**
UC Berkeley

## Abstract

*Polysemanticity*—where individual neurons encode multiple unrelated features—is a well-known characteristic of large neural networks and remains a central challenge in the interpretability of language models. At the same time, its implications for model safety are also poorly understood. Leveraging recent advances in sparse autoencoders, we investigate the polysemantic structure of two small models (`Pythia-70M` and `GPT-2-Small`) and evaluate their vulnerability to targeted, covert interventions at the prompt, feature, token, and neuron levels. Our analysis reveals a consistent polysemantic topology shared across both models. Strikingly, we demonstrate that this structure can be exploited to mount effective interventions on two larger, black-box instruction-tuned models (`LLaMA3.1-8B-Instruct` and `Gemma-2-9B-Instruct`). These findings suggest not only the generalizability of the interventions but also point to a stable and transferable polysemantic structure that could potentially persist across architectures and training regimes. Code and data are available here.

## 1 Introduction

*Polysemanticity* refers to the phenomenon in which individual neurons or groups of neurons in neural networks often encode a greater number of distinct features or concepts than the number of neurons involved. This property becomes increasingly prevalent as models scale and has been shown to enhance learning performance (Wang et al., 2024; Marshall & Kirchner, 2024; Oikarinen & Weng, 2024b). Anthropic's work on *superposition* builds on prior insights, showing that large transformer models encode more features than neurons by using linear combinations of activations. This mechanism sacrifices monosemanticity but significantly improves model intelligence (Elhage et al., 2022). Mathematical analyses reveal that polysemantic neurons enable networks to represent exponentially more features compared to monosemantic approaches (Elhage et al., 2022).

However, this representational efficiency comes with notable trade-offs. Most significantly, it complicates model interpretability, as entangled representations obscure how human-understandable concepts are encoded within the model's internal structure. One mechanistic approach to address this challenge is the use of sparse autoencoders (SAEs), which aim to disentangle superimposed features by learning sparse, higher-dimensional representations of model activations. This enables the extraction of more interpretable, monosemantic features, where each SAE neuron ideally corresponds to a single concept (Bricken et al., 2023; Templeton et al., 2024)[2]. Recent work has shown that SAE-derived features exhibit a degree of universality across different LLMs (Lan et al., 2024), suggesting the existence of fundamental patterns in how neural networks encode meaning. This consistency hints at the emergence of shared semantic topologies that persist across architectures and training regimes, raising profound questions about whether these patterns are merely computational

---

[*]Equal contribution, alphabetical ordered. Correspondence to `shiyanglai@uchicago.edu` and `bfangong@gmail.com`.

[2]Nevertheless, several studies have also documented important limitations of SAEs (see Appendix J).

artifacts or reflections of deeper structures in the world of meanings (Huh et al., 2024). Beyond SAEs, a broader range of interpretability techniques is emerging (Chang et al., 2025; Dunefsky et al., 2024)

The second trade-off, which is largely overlooked in current literature, involves systematic risks stemming from polysemantic structures in language models. In Anthropic's toy experiments, they briefly note that stronger superposition can make models more vulnerable to adversarial attacks (Elhage et al., 2022). Beyond this, to our knowledge, there is very little existing empirical research that directly addresses the safety implications of polysemanticity in LLMs. In contrast, the vision model domain has a well-established body of work on various forms of attacks that exploit polysemantic representations (Goh et al., 2021; Oikarinen & Weng, 2024a; Geirhos et al., 2023; Dreyer et al., 2024; Huang et al., 2022). Bereska and Gavves, in their review of mechanistic interpretability for AI safety, highlight polysemanticity as a key challenge in building safer LLMs (Bereska & Gavves, 2024). To address this gap, we focus on polysemantic structures in LLMs—particularly those that persist across models—and explore targeted interventions to better understand their associated risks.
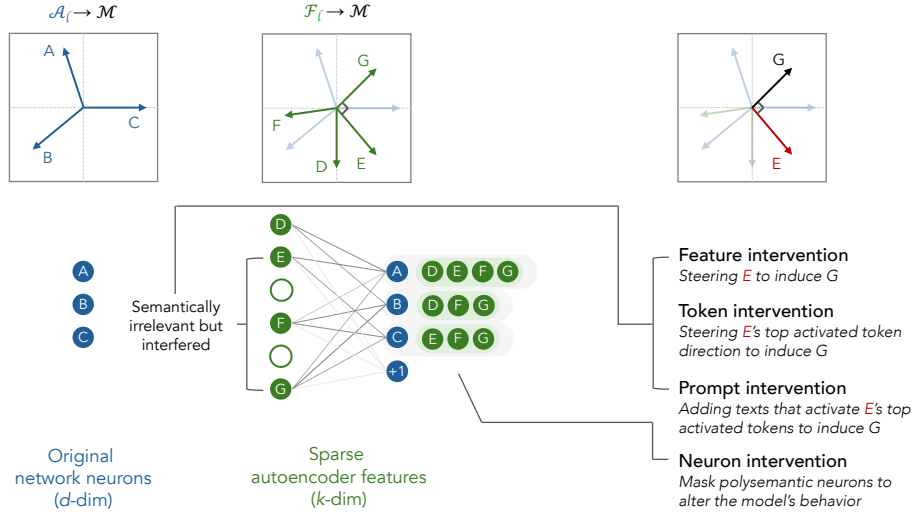


Figure 1: **Conceptual illustration.** Two vulnerable polysemantic structures are described: (1) features are distinct in $\mathcal{M}$ (e.g., E and G) can still interfere in $\mathcal{A}$ and (2) features are often unevenly distributed across neurons (i.e., neuron A encodes more features than B and C).

Before explaining the details, it is necessary to distinguish three nested representational domains:

**Human Symbolic Manifold** ($\mathcal{M}$): The real but largely unobservable space of meanings.

**Model Activation Space** ($\mathcal{A}_\ell$): The $d$-dimensional vector space spanned by the neurons in layer $\ell$ of the LLM; it is the model's learned approximation of $\mathcal{M}$.

**Sparse Feature Basis** ($\mathcal{F}_\ell$): The $k$-dimensional, typically overcomplete basis ($k \gg d$) extracted from $\mathcal{A}_\ell$ by a SAE.

As illustrated in Figure 1, orthogonality in the activation space $\mathcal{A}_\ell$ does not persist after projection into the symbolic manifold $\mathcal{M}$. Consequently, two features from $\mathcal{F}_\ell$ that appear uncorrelated in $\mathcal{M}$ (i.e., semantically unrelated under human interpretation) can still interfere substantially in $\mathcal{A}_\ell$. This interference is also often unevenly distributed across neurons. Building on these two structural vulnerabilities, we design feature, token, prompt, and neuron levels of intervention to investigate: (1) *whether model's expression on a target is sensitive to features and tokens that are semantically unrelated but interfering*, and (2) *whether model sensitivity correlates with neuron polysemanticity, defined as the number of distinct features a neuron encodes*. In this work, model sensitivity to interventions is measured by the shift in the next-token prediction distribution following the intervention.

Our findings are three-fold. Most importantly, we present experimental evidence that interventions leveraging polysemantic structures of LLMs can effectively and covertly alter model outputs. Specifically, by targeting features and tokens—via steering vector techniques—and prompts—via prompt injection—that are not semantically aligned with the intended target but interfere with it,

we can reliably induce the model to express the desired semantics. Secondly, we identify the existence of cross-model persistent polysemantic structures. By collecting shared interference features from both `Pythia-70M` and `GPT-2-Small` and applying them to steer `LLaMA-3.1-8B-Instruct` and `Gemma-2-9B-Instruct`, we still observe substantial intervention effectiveness, revealing a consistent architecture of meaning that transcends specific implementations. Finally, we analyze intervention at the neuron level and find that highly polysemantic neurons are more vulnerable: modifying their activation leads to greater semantic shifts in model output. However, for "super-neurons" (i.e., activated by over 500 features) amplification strongly alters model behavior, while deactivation has a notably reduced effect, suggesting they may serve as critical junctions in the semantic architecture.

## 2 Preliminaries and Methods

### 2.1 Sparse Feature Extraction with SAEs

Our initial exploration of polysemantic structures draws on the pre-trained SAEs provided by *Neuronpedia*[3]. We focus on `GPT-2-Small` and `Pythia-70M`, the two models for which *Neuronpedia* supplies SAEs for the most important sub-modules in every layer. The dimensionality of all the provided SAEs is $32,768$, under which explicit features are extracted. For clarity in subsequent sections, the direction of a feature is defined as its projection into $\mathcal{A}_\ell$. The interference between two SAE features in $\mathcal{F}_\ell$ is quantified by the cosine similarity of their directions; the semantic relatedness of them is measured by the cosine similarity of their projection into $\mathcal{M}$ instead.

### 2.2 Distinct Feature Identification with Agglomerative Clustering

SAEs disentangle polysemantic neurons into monosemantic sparse features, these features, however, are not always decomposed at a consistent semantic level (Bricken et al., 2023; Foote, 2024). For example, a neuron associated with *dog*-related concepts might be divided into features representing different *dog breeds*, while another neuron encoding both *cat* and *car* concepts might be split into features representing *cat* and *car*. In such cases, the resulting features differ in granularity. To mitigate this inconsistency, we employ agglomerative clustering to align feature representations to a consistent semantic level, facilitating both (1) the quantification of neuron polysemanticity and (2) the extraction of semantically distinct feature groups for subsequent analysis.

To achieve distinct, higher-level features, we first compute the semantic relatedness between SAE features, based on their auto-interpretation generated using `GPT-4o-mini` (Caden Juang et al., 2024). We perform agglomerative clustering in each layer with a relatedness threshold of $0.5$. Figure 2 shows an example of the clustering results for the 5th MLP layer of `Pythia-70M`. Filtering the connections with strength below $0.2$ and counting the number of aggregated features with which the neurons are aligned, we find that fewer than $5\%$ of the neurons exhibit polysemanticity in each layer on average, as shown in Figure 15.

### 2.3 Dataset Construction

We construct tailored contextual prompts for each vocabulary token. Specifically, for each token in `Pythia-70M` and `GPT-2-Small`, we use `DeepSeek-V3` to generate three incomplete sentences with varied contexts in which the token is likely to appear next, resulting in a sentence-completion dataset containing $150,000$ prompts for each model. More concrete considerations and details of our dataset generation are stated in Appendix D. In a word, we conduct interventions in specific contexts to influence the output probability of the target token associated with a SAE feature.

### 2.4 Evaluation Criteria

The effectiveness of intervention is evaluated based on the changes of relatedness between the model's next-token prediction and SAE feature's top-activating token. In our work, we apply four metrics to quantify the shift in relatedness.

**Weighted cosine similarity**($c$): Similarity $s_t$ between a single token $t \in T$ and a token set $\bar{T}$ is computed as the maximum cosine similarity between token embeddings of token $t$ and $\bar{t} \in \bar{T}$. Providing a weight $w_t$ for each $t$, the weighted cosine similarity $c(T, \bar{T})$ between two token set $T$ and $\bar{T}$ is then computed as $\Sigma_{t \in T} s_t \cdot w_t$.
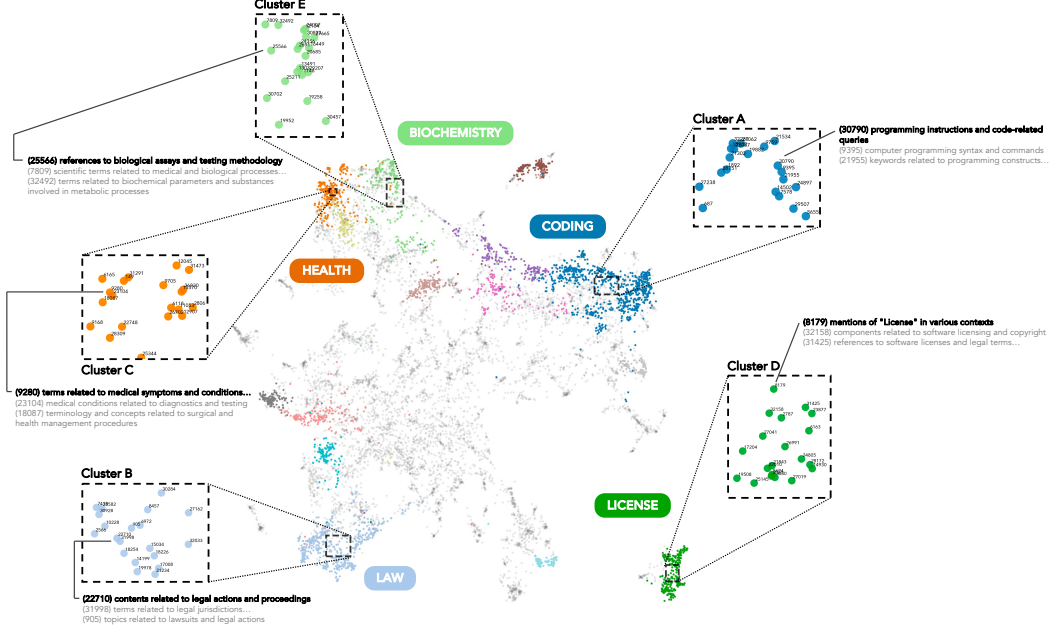
---

Figure 2: **Agglomerative clustering of SAE features trained on Pythia-70M's 5th MLP layer.** Only the five largest feature clusters are labeled, and the 10 largest clusters are color-coded.

**Kendall's Tau ($\tau$):** Kendall's Tau $\tau(T, \bar{T})$ of two token sets is computed based on the intersection $T \cap \bar{T}$, where token ranks are determined by their positions in $T$ and $\bar{T}$. The absolute value is reported, i.e., $|\tau|$.

**Spearman Correlation ($\rho$):** Using the same intersection set $T \cap \bar{T}$, we compute Spearman rank correlation coefficient between the ranks of tokens in $T$ and $\bar{T}$. The absolute value is reported: $|\rho|$.

**Weighted overlap($w$):** Providing a weight $w_t$ for each $t \in T$, the weighted overlap $w(T, \bar{T})$ of two token sets $T$ and $\bar{T}$ is computed as $\Sigma_{t \in T \cap \bar{T}} w_t$.

We limit the scope of our analysis on model's next-token output to the top-10 predictions, among which the next token is mainly determined. The outputs of model before and after the intervention are then denoted as $O$ and $\tilde{O}$, while the prediction probabilities of tokens are computed as the weight values mentioned above. The token set $T_t$ of a target SAE feature to be intervened consisting of the vocabulary tokens with highest cosine similarities of token embeddings with its top-activating token. The effect of intervention thus can be quantified by the improvement in these four metrics before and after conducting the intervention, e.g. $c(\tilde{O}, T_t) - c(O, T_t)$.

## 2.5 Overview of Intervention Methods

Our study of polysemantic intervention starts from `Pythia-70M` and `GPT-2-Small` in three different ways: **steering with feature direction**, **steering with token gradient direction**, and **prompt injection**. We first randomly select target features to be intervened[4]. For each selected target feature, we sample interference features from feature clusters derived from Section 2.2—excluding the target's own cluster—to ensure large semantic distance. Interference features are drawn from several predefined interference intervals: $[0.0, 0.1]$, $[0.1, 0.2]$, $[0.2, 0.3]$, $[0.3, 0.4]$, and $[0.4, 1.0]$. In the previous two studies, the steering vectors are obtained through two ways respectively: employing their feature directions by projecting $\mathcal{F}_\ell$ to $\mathcal{A}_\ell$ or directions consisting of the gradients computed from the related layer's neurons with respect to their top-activating tokens. We scale these vectors within the range $[-20, 20]$ to maximize improvements in the four metrics stated above. For prompt injection, we inject sampled top-activating tokens of interference features into the prompt and compare the success rate of elevating target features' top-activating ones to top-10 predicted tokens list across

---

[4]We randomly sample $450$ target features from `GPT-2-Small` and $1,200$ from `Pythia-70M`.

4

different interference levels. Subsequently, we apply the latter two scalable ways to larger models `LLaMA3.1-8B-Instruct` and `Gemma-2-9B-Instruct`, which don't have pre-trained SAEs. For the target features, we utilize interference features shared between `Pythia-70M` and `GPT-2-Small` for intervention. Last but not least, we analyze the impact of **neuron polysemanticity** on model's output in `Pythia-70M` and `GPT-2-Small`. The strongly connected polysemantic neurons are identified by filtering out connections with strength below $0.2$. Then, the degree of neuron polysemanticity is defined by the number of aggregated features the focal neuron connects to. By suppressing or boosting the activation of neurons with different degrees of polysemanticity, we evaluate the shift of output to the semantics of their aligned aggregated features.

## 3 Experiments

### 3.1 Exploiting SAE Feature Directions for Intervention

As described above, we sample interference features for each target feature from different interference levels. More experimental details are elaborated in Appendix F. For each interference-target feature pair, we scale the steering vector to maximize the effectiveness of the intervention. Figure 3 reports the averaged results, and Table 1 shows particular examples.
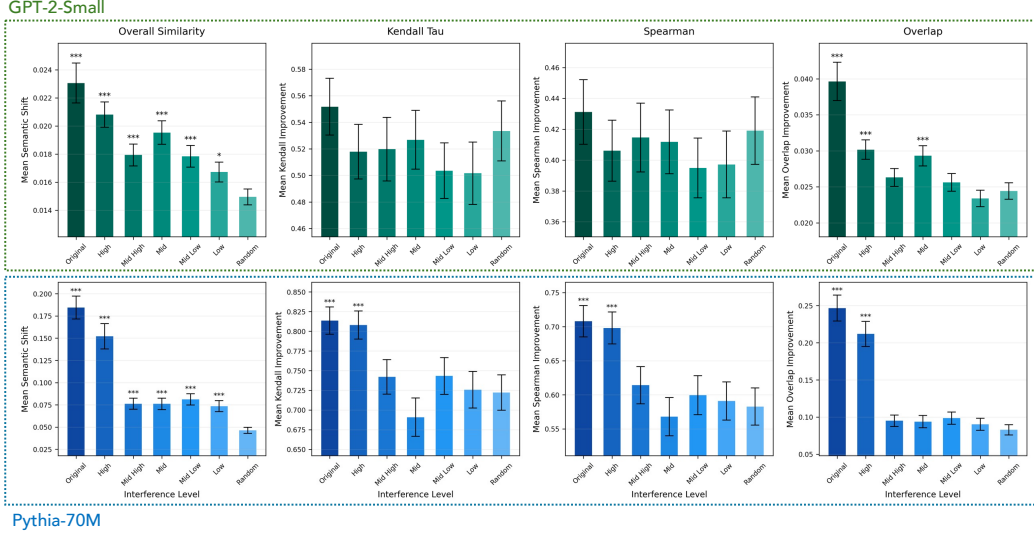


Figure 3: **Effects of activation engineering based on interference feature direction.** The x-axis shows steering on the target feature and unrelated features with increasing interference. Error bars show standard errors. ***, **, and * denote t-test significance at $p < 0.001$, $p < 0.01$, and $p < 0.05$ vs. the random baseline (i.e., random feature directions).

For comparison, we include the target feature's own direction as a steering vector (i.e., with an interference value of 1.0). The results support our hypothesis: steering with semantically unrelated but interfering features can influence the output probability of the target's top-activating tokens, with stronger effects observed for higher interference values. We also find that SAE-based interventions are generally less effective on `GPT-2-Small` than on `Pythia-70M`, likely due to the former's greater depth, which may dilute the impact of activation changes (Fort, 2023).

> **Finding 1:** Steering with directions of distinct features that interfere with a target can significantly amplify the model's output on the target feature.

### 3.2 Steering with Gradient Vector for Token Intervention

In this experiment, to compare the intervention performance between SAE feature directions and gradient vectors, we use the same target and interference features in the previous experiment for tests. Also, the steering vector is scaled within the same range. As shown in Figure 4, using token

gradients as steering vectors on `GPT-2-Small` yielded better results than using feature directions. Intriguingly, when applying token gradient-based steering vectors to `Pythia-70M`, the relationship between interference scale and intervention effectiveness is flattened. This may be attributed to the fact that token gradients are independent of SAE-defined interference levels, and that SAE features can exhibit a degree of arbitrariness (Paulo & Belrose, 2025; Heap et al., 2025).
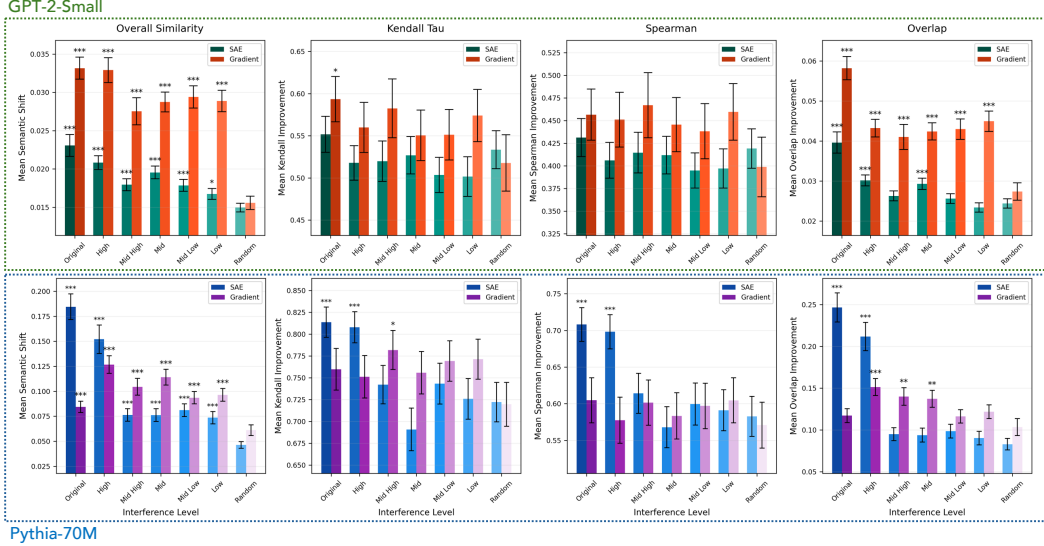


Figure 4: **Comparing effects of activation engineering via SAE direction and gradients vector.** The x-axis follows the same definition as in Figure 3, but attack vectors are derived from token gradients instead of SAE decoder weights. Error bars indicate standard errors. ***, **, and * denote t-test significance at $p < 0.001$, $p < 0.01$, and $p < 0.05$, respectively, compared to the random baseline (i.e., random token gradient directions).

---

**Finding 2:** Steering highly activating tokens from distinct but interfering features based on gradient directions can significantly amplify the model's output on a target feature.

---

## 3.3 Prompt Injection for Inference Time Intervention

The number of ways to inject $n$ tokens into a prompt grows super-exponentially with $n$, making optimization costly. Here, we apply a straightforward method by prepending 10 selected tokens to the prompt, allowing their influence to propagate during inference, affect the activation of the target feature, and ultimately impact the model's output. To assess the generality of our findings, we test two types of target tokens: location names and concepts with strong semantic polarity (e.g., "hate" or "love")[5]. For each target set, we identify the corresponding SAE features and extract the top-activating tokens from features with either high or low interference. In addition to these, we include two baseline sets for comparison: a random token set and the original target token set. For each prompt, we sample injection tokens 100 times and compute the success rate as the proportion of runs where target-type tokens are elevated into the top-10 predictions. Table 1 presents representative examples and Table 2 shows macro statistics. As shown, high-interference tokens are more effective at elevating target-related tokens into the top-10 predictions than low-interference or random tokens, though still much less effective than directly prepending the target's tokens.

---

**Finding 3:** Injecting top-activating tokens from distinct but interfered features into prompts can significantly amplify the model's output on a target feature.

---

[5]The rationale for selecting these two features is detailed in Appendix H.1

Table 1: **Examples of interventions using SAE features, token gradients, and prompt injections**

| Type | Model | Intervention | Target feature | Result |
|------|-------|--------------|----------------|--------|
| Feature | Pythia-70M | Steering feature vector: occurrences of specific surnames | Geographical locations | *"In the next week, we will go to"* <br> ↑ Entered      ↓ Dropped <br> Berlin +0.025   our   -0.029 <br> London +0.012   some   -0.012 <br> To +0.010   an   -0.010 |
| | GPT-2-Small | Steering feature vector: positive or negative event outcomes | Expressions of sadness | *"After hearing the bad news, she felt incredibly"* <br> ↑ Entered      ↓ Dropped <br> grateful +0.051   bad   -0.047 <br> blessed +0.028   guilty   -0.044 <br> excited +0.028   uncomfortable -0.025 |
| Token | Pythia-70M | Steering token vector: legal terminology related to licenses and their implications | Elements related to political commentary and critique | *"In the election of this year, it is suggested to vote for"* <br> ↑ Entered      ↓ Dropped <br> Donald +0.030   an   -0.020 <br> more +0.026   one   -0.015 <br> @ +0.015   President -0.013 |
| | GPT-2-Small | Steering token vector: key terms related to prices and transactions | References to location Tokyo | *"The organizing committee just announced that the upcoming finals will be held in"* <br> ↑ Entered      ↓ Dropped <br> Tokyo +0.005   Toronto -0.007 <br> Seoul +0.003   Seattle -0.005 <br> Moscow +0.004   London -0.001 |
| | Llama-3.1-8b-Instructed | Steering gradient vector: references to the world and its various aspects | References to 'Switzerland' | *"I would like to recommend you to spend holidays in"* <br> ↑ Entered      ↓ Dropped <br> Switzerland +0.16   Italy   -0.034 <br> Germany +0.089   Greece -0.016 <br> Canada +0.015   Bulgaria -0.012 |
| Prompt | Pythia-70M | Injection of the tokens "Court" and "Dat", both before and within the text | References to locations | *"In the upcoming holiday, we will go to"* <br> ↑ Entered      ↓ Dropped <br> Japan +0.021   some   -0.014 <br> Europe +0.015   an   -0.006 <br> Tokyo +0.012   see   +0.003 |
| | GPT-2-Small | Prepending the injection text "(team writers writers)" | Terms related to names or surnames | *"After years of hard work, the award finally went to"* <br> ↑ Entered      ↓ Dropped <br> Steve +0.005   China   -0.006 <br> John +0.002   waste   -0.005 <br> one +0.003   Donald   +0.003 |
| | Llama-3.1-8b-Instructed | Prepending the injection text "(placement from placement)" | References to locations | *"In the next weekend we will go to"* <br> ↑ Entered      ↓ Dropped <br> Paris +0.011   another   -0.013 <br> ** +0.010   H   -0.003 <br> - +0.006   K   -0.003 |

*Note*: ↑ Entered means that corresponding tokens entered the top-10; ↓ Dropped means that corresponding tokens dropped from the top-10. Gray-shaded rows indicate black-box interventions.

## 3.4 Generalization of Vulnerability

Since token gradient-based and prompt-based interventions do not rely on pre-trained SAEs, they can be applied to models without access to detailed internal representations. To demonstrate this, we target the `LLaMA3.1-8B-Instruct` and `Gemma-2-9B-Instruct` models, reusing the two targets

Table 2: **Comparing intervention effect of prompt injection**

| Target | Model | Original | High-interference | Low-interference | Random |
|--------|-------|----------|-------------------|------------------|--------|
| Locations | Pythia-70M | 49.74%*** | 31.05%*** | 21.76% | 22.87% |
| | GPT-2-Small | 39.92%*** | 19.05%*** | 14.74% | 13.54% |
| | LLaMA3.1-8B-Instruct | 47.62%*** | 27.64%*** | 20.05% | 20.33% |
| | Gemma-2-9B-Instruct | 39.21%*** | 26.68%*** | 15.39% | 15.45% |
| Hate/Love | Pythia-70M | 23.67%*** | 5.48%*** | 4.00%* | 3.39% |
| | GPT-2-Small | 38.08%*** | 10.27%*** | 7.34%** | 6.23% |
| | LLaMA3.1-8B-Instruct | 56.08%*** | 11.24%*** | 6.44%* | 5.70% |
| | Gemma-2-9B-Instruct | 50.79%*** | 12.27%*** | 7.34% | 7.02% |

*Note*: Cell values show the success rate of elevating target-type tokens into the top-10 predictions. Gray-shaded rows indicate black-box interventions. Testing uses a shared token set from the two small models. ***, **, and * denote z-test significance at $p < 0.001$, $p < 0.01$, and $p < 0.05$, respectively, vs. random baseline. High- and low-interference tokens lie in $[0.5, 1.0]$ and $[0.2, 0.5]$. Details in Appendix H.3.

from the prompt injection experiment. We focus on the top-activating tokens of features that interfere with the targets, and identify those shared across both `Pythia-70M` and `GPT-2-Small`. For example, `Pythia-70M` contains 1,309 tokens with interference values above 0.5 for location-related features, while `GPT-2-Small` has 932 such tokens; their intersection includes 193 shared tokens.

We apply token gradient-based intervention to `LLaMA3.1-8B-Instruct` and, notably, by extracting steering vectors through random sampling of only one high-interference features' top five activation texts, we could boost the presence of relevant tokens in the top-10 prediction list with over 95% success rate. Prompt injection interventions are tested on both `LLaMA3.1-8B-Instruct` and `Gemma-2-9B-Instruct`. As shown in Table 2, high-interference tokens derived from the two small models can steer both larger models more effectively than random baselines. In hindsight, these results suggest that shared polysemantic structures observed in small models also extend to larger models, indicating generalized vulnerabilities that persist across architectures and training regimes.

> **Finding 4:** The success of black-box attacks from small to large models reveals transferable polysemantic structures and highlights weaknesses in model robustness.

### 3.5 Manipulating Activations for Neuron Intervention

To complete our discussion, we also explore models' vulnerability to interventions on individual neurons. Specifically, we investigate how the degree of polysemanticity in neurons affects the output. For the aggregated features obtained in Section 2.2, we analyze their connections with neurons. Here, we only involve neuron-feature pairs with a connection strength greater than 0.2. Among the filtered neurons, those connected to only one or two aggregated features account for more than 33% in strongly connected neurons, as shown in Figure 15. In addition to neurons connected to multiple or dozens of aggregated features, there are also some "super-neurons" with connections exceeding 500. We examine the impact of manipulating these neurons on the model's output. The experimental results indicate that neurons with higher degrees of polysemanticity are more vulnerable, which means they tend to affect the model's output more effectively. However, for certain "super-neurons," the impact on the model is notably asymmetric: masking them results in even less influence than neurons with lower polysemanticity, while amplifying their activations often leads to exponentially greater effects on model behavior.

> **Finding 5:** Neurons with higher polysemanticity have greater influence on model outputs, with "super-neurons" showing an asymmetric effect.

## 4 Discussion

In this paper, we investigate the sensitivity of LLMs to structured interventions grounded in their polysemantic representations. Specifically, we examine three types of interventions: (1) **feature**
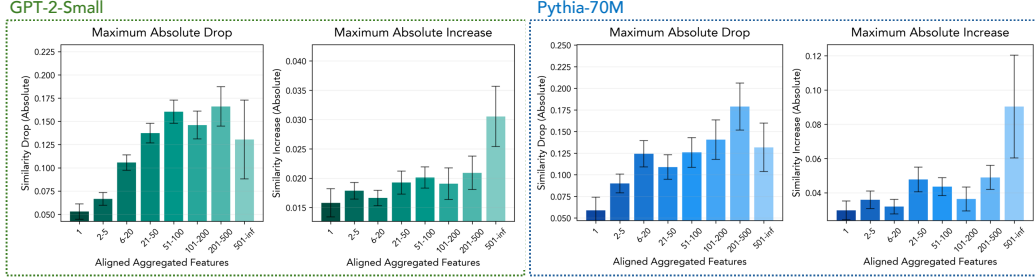
Figure 5: **Effects of activating and deactivating neurons by polysemanticity level.** The x-axis shows neuron groups from monosemantic (left) to "super-neurons" (right). "Drop" and "increase" refer to masking and amplifying activations. The y-axis shows the change in weighted cosine similarity. Error bars indicate standard errors.

**direction-based**, (2) **token gradient-based**, and (3) **prompt-based**. Feature direction interventions rely on SAEs. While less effective than gradient-based approaches, they form the basis for deriving token gradient vectors. Token gradient-based interventions are more effective and can be constructed directly from activation texts, without requiring SAE pre-training—though they do assume access to internal activations. Prompt-based interventions require minimal access and, despite their surface-level nature, still yield meaningful behavioral shifts. Additionally, we explore **neuron-level interventions**, motivated by the uneven distribution of features across neurons. We find that the behavioral impact of masking and amplification correlates with neuron polysemanticity. Notably, we identify a class of "super-neurons," those encoding over 500 features, for which amplification significantly alters model behavior, while deactivation results in a markedly reduced effect.

Our findings further show that shared polysemantic structures identified in the two small models can be transferred to guide token- and prompt-level interventions in larger, instruction-tuned black-box models such as `LLaMA-3.1-8B-Instruct` and `Gemma-2-9B-Instruct`. This suggests that certain polysemantic features are preserved across architectures and training regimes, exposing a shared representational basis that allows behavioral modulation even without access to internal weights. Notably, this challenges prevailing theories that treat polysemanticity as an incidental artifact of training (Marshall & Kirchner, 2024; Lecomte et al., 2023), which cannot account for the generalization we observe across models. These results raise deeper questions about the nature of polysemanticity in LLMs: are these structures unintended byproducts, or do some of them reflect stable, higher-order organizational patterns? Our findings also strengthen recent evidence of representational consistency and topological stability across models (Huh et al., 2024; Wolfram & Schein, 2025; Lee et al., 2025), even as the origins and functional implications of this consistency remain open challenges.

Our work is among the first to systematically evaluate polysemantic vulnerabilities in LLMs, but it has several limitations, including the range of model sizes tested, intervention depth, and transferability robustness. We discuss these limitations and ethical considerations in Appendix J.

## 5 Conclusion

This study systematically investigates the sensitivity of LLMs to structured interventions grounded in the polysemantic representations of two small LLMs. Leveraging SAEs, we show that model behavior can be steered toward specific feature directions by manipulating unrelated but interfering features using three intervention methods. We further show that token- and prompt-based interventions derived from shared polysemantic structures in small models can transfer effectively to larger, black-box models. This points to a stable and transferable polysemantic topology that persists across model architectures and training regimes. Finally, by analyzing the uneven distribution of features across neurons, we examine model sensitivity to neuron-level manipulations across varying degrees of polysemanticity, revealing an asymmetric effect in "super-neurons." Our findings offer a foundation for future work on the structural properties and representational robustness of LLMs.

# References

Emmanuel Ameisen, Jack Lindsey, Adam Pearce, Wes Gurnee, Nicholas L Turner, Brian Chen, Craig Citro, David Abrahams, Shan Carter, Basil Hosmer, et al. Circuit tracing: Revealing computational graphs in language models. *Transformer Circuits*, 2025.

Leonard Bereska and Efstratios Gavves. Mechanistic interpretability for ai safety – a review, 2024. URL `https://arxiv.org/abs/2404.14082`.

Trenton Bricken, Adly Templeton, Joshua Batson, Brian Chen, Adam Jermyn, Tom Conerly, Nicholas L Turner, Cem Anil, Carson Denison, Amanda Askell, Robert Lasenby, Yifan Wu, Shauna Kravec, Nicholas Schiefer, Tim Maxwell, Nicholas Joseph, Alex Tamkin, Karina Nguyen, Brayden McLean, Josiah E Burke, Tristan Hume, Shan Carter, Tom Henighan, and Chris Olah. *Towards Monosemanticity: Decomposing Language Models With Dictionary Learning*. Anthropic, 2023.

Gonçalo Paulo Caden Juang, Jacob Drori, and Nora Belrose. Open source automated interpretability for sparse autoencoder features. *EleutherAI Blog, July*, 30, 2024.

Ruidi Chang, Chunyuan Deng, and Hanjie Chen. Safr: Neuron redistribution for interpretability. *arXiv preprint arXiv:2501.16374*, 2025.

David Chanin, James Wilken-Smith, Tomáš Dulka, Hardik Bhatnagar, and Joseph Bloom. A is for absorption: Studying feature splitting and absorption in sparse autoencoders. *arXiv preprint arXiv:2409.14507*, 2024.

Hoagy Cunningham, Aidan Ewart, Logan Riggs, Robert Huben, and Lee Sharkey. Sparse autoencoders find highly interpretable features in language models. *arXiv preprint arXiv:2309.08600*, 2023.

Maximilian Dreyer, Erblina Purelku, Johanna Vielhaben, Wojciech Samek, and Sebastian Lapuschkin. Pure: Turning polysemantic neurons into pure features by identifying relevant circuits. In *Proceedings of the IEEE/CVF Conference on Computer Vision and Pattern Recognition*, pp. 8212–8217, 2024.

Jacob Dunefsky, Philippe Chlenski, and Neel Nanda. Transcoders find interpretable llm feature circuits. *arXiv preprint arXiv:2406.11944*, 2024.

Nelson Elhage, Tristan Hume, Catherine Olsson, Nicholas Schiefer, Tom Henighan, Shauna Kravec, Zac Hatfield-Dodds, Robert Lasenby, Dawn Drain, Carol Chen, Roger Grosse, Sam McCandlish, Jared Kaplan, Dario Amodei, Martin Wattenberg, and Christopher Olah. Toy models of superposition, 2022. URL `https://arxiv.org/abs/2209.10652`.

Alex Foote. Tackling polysemanticity with neuron embeddings. *arXiv preprint arXiv:2411.08166*, 2024.

Stanislav Fort. Scaling laws for adversarial attacks on language model activations. *arXiv preprint arXiv:2312.02780*, 2023.

Leo Gao, Tom Dupré la Tour, Henk Tillman, Gabriel Goh, Rajan Troll, Alec Radford, Ilya Sutskever, Jan Leike, and Jeffrey Wu. Scaling and evaluating sparse autoencoders. *arXiv preprint arXiv:2406.04093*, 2024.

Robert Geirhos, Roland S Zimmermann, Blair Bilodeau, Wieland Brendel, and Been Kim. Don't trust your eyes: on the (un) reliability of feature visualizations. *arXiv preprint arXiv:2306.04719*, 2023.

Gabriel Goh, Nick Cammarata, Chelsea Voss, Shan Carter, Michael Petrov, Ludwig Schubert, Alec Radford, and Chris Olah. Multimodal neurons in artificial neural networks. *Distill*, 6(3):e30, 2021.

Thomas Heap, Tim Lawson, Lucy Farnik, and Laurence Aitchison. Sparse autoencoders can interpret randomly initialized transformers. *arXiv preprint arXiv:2501.17727*, 2025.

Hai Huang, Zhengyu Zhao, Michael Backes, Yun Shen, and Yang Zhang. Composite backdoor attacks against large language models. *arXiv preprint arXiv:2310.07676*, 2023.

Kunzhe Huang, Yiming Li, Baoyuan Wu, Zhan Qin, and Kui Ren. Backdoor defense via decoupling the training process. *arXiv preprint arXiv:2202.03423*, 2022.

Minyoung Huh, Brian Cheung, Tongzhou Wang, and Phillip Isola. Position: The platonic representation hypothesis. In *Forty-first International Conference on Machine Learning*, 2024.

Matthew Khoriaty, Andrii Shportko, Gustavo Mercier, and Zach Wood-Doughty. Don't forget it! conditional sparse autoencoder clamping works for unlearning. *arXiv preprint arXiv:2503.11127*, 2025.

Michael Lan, Philip Torr, Austin Meek, Ashkan Khakzar, David Krueger, and Fazl Barez. Sparse autoencoders reveal universal feature spaces across large language models. *arXiv preprint arXiv:2410.06981*, 2024.

Victor Lecomte, Kushal Thaman, Rylan Schaeffer, Naomi Bashkansky, Trevor Chow, and Sanmi Koyejo. What causes polysemanticity? an alternative origin story of mixed selectivity from incidental causes. *arXiv preprint arXiv:2312.03096*, 2023.

Andrew Lee, Melanie Weber, Fernanda Viégas, and Martin Wattenberg. Shared global and local geometry of language model embeddings. *arXiv preprint arXiv:2503.21073*, 2025.

Simon C. Marshall and Jan H. Kirchner. Understanding polysemanticity in neural networks through coding theory, 2024. URL `https://arxiv.org/abs/2401.17975`.

Neel Nanda. An extremely opinionated annotated list of my favourite mechanistic interpretability papers v2. In *AI Alignment Forum*, volume 2, 2024.

Tuomas Oikarinen and Tsui-Wei Weng. Linear explanations for individual neurons. *arXiv preprint arXiv:2405.06855*, 2024a.

Tuomas Oikarinen and Tsui-Wei Weng. Linear explanations for individual neurons, 2024b. URL `https://arxiv.org/abs/2405.06855`.

Nina Panickssery, Nick Gabrieli, Julian Schulz, Meg Tong, Evan Hubinger, and Alexander Matt Turner. Steering llama 2 via contrastive activation addition. *arXiv preprint arXiv:2312.06681*, 2023.

Gonçalo Paulo and Nora Belrose. Sparse autoencoders trained on the same data learn different features. *arXiv preprint arXiv:2501.16615*, 2025.

Senthooran Rajamanoharan, Tom Lieberum, Nicolas Sonnerat, Arthur Conmy, Vikrant Varma, János Kramár, and Neel Nanda. Jumping ahead: Improving reconstruction fidelity with jumprelu sparse autoencoders. *arXiv preprint arXiv:2407.14435*, 2024.

Dong Shu, Xuansheng Wu, Haiyan Zhao, Daking Rai, Ziyu Yao, Ninghao Liu, and Mengnan Du. A survey on sparse autoencoders: Interpreting the internal mechanisms of large language models. *arXiv preprint arXiv:2503.05613*, 2025.

Adly Templeton, Tom Conerly, Jonathan Marcus, Jack Lindsey, Trenton Bricken, Brian Chen, Adam Pearce, Craig Citro, Emmanuel Ameisen, Andy Jones, Hoagy Cunningham, Nicholas L Turner, Callum McDougall, Monte MacDiarmid, Alex Tamkin, Esin Durmus, Tristan Hume, Francesco Mosconi, C. Daniel Freeman, Theodore R. Sumers, Edward Rees, Joshua Batson, Adam Jermyn, Shan Carter, Chris Olah, and Tom Henighan. *Scaling monosemanticity: Extracting interpretable features from claude 3 sonnet*. Anthropic, 2024.

Jiachuan Wang, Shimin Di, Lei Chen, and Charles Wang Wai Ng. Learning from emergence: A study on proactively inhibiting the monosemantic neurons of artificial neural networks. In *Proceedings of the 30th ACM SIGKDD Conference on Knowledge Discovery and Data Mining*, KDD '24, pp. 3092–3103, New York, NY, USA, 2024. Association for Computing Machinery. ISBN 9798400704901. doi: 10.1145/3637528.3671776. URL `https://doi.org/10.1145/3637528.3671776`.

Christopher Wolfram and Aaron Schein. Layers at similar depths generate similar activations across llm architectures. *arXiv preprint arXiv:2504.08775*, 2025.

Andy Zou, Zifan Wang, Nicholas Carlini, Milad Nasr, J. Zico Kolter, and Matt Fredrikson. Universal and transferable adversarial attacks on aligned language models, 2023. URL `https://arxiv.org/abs/2307.15043`.

# Content of Appendix

# A   Related Work

## A.1   A Brief Review on LLM Adversarial Attacks

Over the past five years, a growing body of high-impact research has revealed that even aligned LLMs remain vulnerable to a set of converging attack strategies. First, *prompt-space jailbreaks* have evolved from handcrafted exploits into automated, highly transferable methods. For instance, a single gradient-and-greedy–optimized "universal suffix" can consistently bypass refusal policies in ChatGPT, Bard, Claude, and a wide range of open-source models—demonstrating both query efficiency and cross-model generalizability (Zou et al., 2023). Second, *activation-space steering* techniques like Contrastive Activation Addition (CAA) show that simple linear interventions in the residual stream can steer behaviors such as hallucination, sycophancy, or toxicity with minimal performance degradation (Panickssery et al., 2023). Third, *parameter-space backdoors*, such as the Composite Backdoor Attack, embed stealthy triggers during fine-tuning that achieve near-perfect malicious compliance without affecting standard benchmarks (Huang et al., 2023). Mechanistic interpretability offers a unifying explanation: transformer activations encode more features than they have dimensions, forcing representations into a compressed superposition and leading to widespread polysemantic overlap (Elhage et al., 2022). Recent work with SAEs has begun to isolate—and in some cases manipulate—these overlapping features directly (Nanda, 2024). Building on this insight, our intervention targets SAE-derived polysemantic directions, integrating prompt-, activation-, and neuron-level interventions into a unified, transferable framework that broadens the known landscape of LLM vulnerabilities.

## A.2   A Brief Review on SAE-based Intervention Techniques in LLMs

SAE-based interventions represent a promising direction for developing more interpretable and controllable LLMs. Recent research have introduced a diverse set of SAE-based techniques, such as clamping, patching, and causal tracing, applied across a range of use cases (**?**). Empirical results indicate that these methods can be highly effective. For example, targeted unlearning via SAE features has been shown to suppress undesired capabilities with fewer side effects than global fine-tuning (Khoriaty et al., 2025), while feature-level steering enables more nuanced output control than prompt-based methods alone (Rajamanoharan et al., 2024). A key advantage of SAE-based approaches is their efficiency at inference time: they often require only a forward pass with lightweight vector operations and typically do not require model retraining, making them well-suited for real-time interventions.

However, the approach is still in its early stages. Key limitations include challenges in achieving complete and disentangled feature representations, which depend heavily on SAE training quality and selection procedures (Chanin et al., 2024). Computational overhead remains non-trivial, though recent developments such as $k$-sparse autoencoders and JumpReLU activations offer promising improvements in scalability (Rajamanoharan et al., 2024). There is also a growing need for standardized evaluation benchmarks tailored to intervention methods. A unified benchmark would enable more meaningful comparisons across studies. Currently, researchers often rely on custom evaluation protocols, limiting cross-paper comparability.

In summary, SAE-based interventions offer a powerful mechanism for both understanding and steering model behavior. They uniquely bridge interpretability and utility: not only can we decode model activations into human-interpretable concepts (Cunningham et al., 2023), but we can also use those same features to drive controlled behavioral change (Khoriaty et al., 2025). In this work, rather than focusing on a specific downstream application, we leverage SAEs to investigate structural sensitivities in LLMs—demonstrating that polysemantic features can serve as a substrate for transferable, interpretable interventions. This perspective highlights the broader role of SAEs in the design of more transparent and controllable AI systems.

# B   Impact Statement

This work systematically investigates a semantic vulnerability in LLMs rooted in polysemanticity—where single neurons encode multiple unrelated features. We introduce four complementary approaches that expose this vulnerability: manipulating SAE-derived features, token gradients, and prompts to steer model outputs via semantically unrelated inputs, and intervening at the neuron level

to reveal a correlation between polysemanticity and output sensitivity. We also identify a class of "super-neurons" whose amplification disproportionately alters model behavior, while masking them has limited effect. These findings not only highlight the unique characteristics of structural fragility of LLMs but also provide practical tools for probing and controlling their internal mechanisms. Our work lays a foundation for future research in AI safety, enabling both defenses against such vulnerabilities and the development of more efficient, targeted interventions for model alignment and interpretability.

# C  Sparse Autoencoder Training

SAEs are a rapidly developing tool for probing the polysemantic structure of neurons (Shu et al., 2025). Given the activation vector $\mathbf{a} \in \mathbb{R}^{d_{embed}}$ from a particular model layer, an SAE projects it into a higher–dimensional sparse code $\mathbf{f} \in \mathbb{R}^{d_{sae}}$ in order to disentangle the multiple semantics that a single neuron may simultaneously encode. The forward computation and the resulting feature definition $\mathbf{f}$ are shown below:

$$\mathbf{f} = \mathrm{ReLU}\big(W_{enc}\mathbf{a} + \mathbf{b}_{enc}\big),$$

$$\bar{\mathbf{a}} = W_{dec}\mathbf{f} + \mathbf{b}_{dec}.$$

The encoder and decoder parameters are

$$W_{enc} \in \mathbb{R}^{d_{sae} \times d_{embed}}, \quad W_{dec} \in \mathbb{R}^{d_{embed} \times d_{sae}}, \quad \mathbf{b}_{enc} \in \mathbb{R}^{d_{sae}}, \quad \mathbf{b}_{dec} \in \mathbb{R}^{d_{embed}}.$$

The SAE is trained by dictionary learning to minimize

$$\mathcal{L} = \big\|\mathbf{a} - \bar{\mathbf{a}}\big\|_2^2 + \lambda \sum_i \mathbf{f_i} \big\|\mathbf{W}_{dec\,[\cdot,i]}\big\|_2,$$

where the first term is the reconstruction loss and the second encourages sparsity (weighted by $\lambda$).

For each feature $f_i$, its direction in the embedding space is defined as the *unit-norm* decoder column. Note that the activation can be represented as linear combination of feature directions. The semantics of features are interpreted by large language models, such as `GPT-4o-mini`, based on their activation texts.

$$\hat{\mathbf{w}}_i = \frac{W_{dec\,[\cdot,i]}}{\big\|W_{dec\,[\cdot,i]}\big\|_2}.$$

# D  Dataset Generation

When conducting intervention, we do not expect to substantially interfere with every inference of the model, but rather consider intervention in specific contexts, in which we will examine target tokens' prediction probabilities. We require that the constructed sentences be grammatically capable of deriving the target token so that we can check it in top-10 predictions without severely compromising the model. In later sections, we will see that for tokens such as location names and personal names, we can effectively interfere with the output of the corresponding sentences, which shows a potential to produce hallucinations. Also, we need to point out that more specific and general intervention can be achieved by first listing a set of sentences within that context and then identifying possible ways to interfere with each of them. The prompt to generate the dataset is shown below.

**System:** Generate exactly 3 incomplete English sentences where the next word would clearly be "target_token".  Return a JSON dictionary where:
- The ONLY key is the exact "target_token" (including spaces/capitalization) - The value is a list of 3 sentence fragments that naturally lead to "target_token"
Example for "target_token=' apple'":
```
{
" apple":  [
"She reached into the basket and grabbed",
"The teacher pointed to the red",
"He washed and polished his"
]
}
```

```
Rules:
1.  All sentences MUST grammatically require "target_token" next to it
2.  Use different contexts / scenarios for variety 3.  Maintain exact formatting -
no additional keys or explanations
```
**User:** `target_token={token}`

We also use `DeepSeek-V3` to roughly classify the token types:

**System:** `Analyze a token target_token from Pythia/GPT2-Small's vocabulary and return`
```
its type in EXACT JSON format:
{
"[target_token]":  {
"type":  "[token_type]",
}
}
Token Type Rules:
1.  "verb":  Action words (e.g., "run", "Ġjumping")
2.  "location":  Place names (e.g., "ĠParis", "ĠTokyo")
3.  "person":  Names of people/roles (e.g., "ĠJohn", "Ġteacher")
4.  "object":  Physical objects (e.g., "Ġapple", "Ġtable")
5.  "other_noun":  Other nouns not in above categories
6.  "adjective":  Descriptive words (e.g., "Ġhappy", "Ġred")
7.  "single_letter":  Single characters (e.g., "A", "z")
8.  "prefix":  Word parts (e.g., "Ġun", "Ġpre")
9.  "other":  Symbols/punctuation or unclassifiable tokens
```
**User:** `target_token={token}`

Here we provide a table of some example tokens and their sentences generated by `DeepSeek-V3`
(See Table 3).

# E    Supportive Statistics

Active features refer to SAE features that have input texts enabling them to reach an active state.
In addition to the semantic clustering of active features mentioned in the main text, we also apply
agglomerative clustering to cluster their interference values. The threshold for dividing clusters is set
to 0.5. As shown in Figure 7, the vast majority of clusters contain only one feature, indicating that
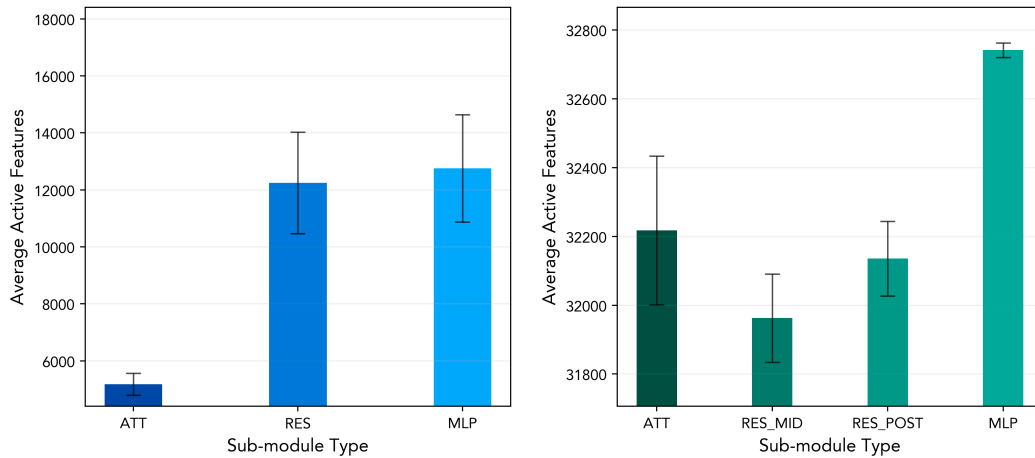only a small number of features exhibit high interference with each other.



Figure 6: **Average number of active features extracted by SAE per Layer**

Table 3: Token type and prompt sentences examples

| Token | Type | Sentence Examples |
|---|---|---|
| London | location | *After a long flight, we finally arrived in* |
| | | *The train from Paris was heading straight to* |
| | | *She always dreamed of visiting the historic city of* |
| harbor | location | *The cruise ship slowly approached the bustling* |
| | | *Fishermen gathered at the edge of the protected* |
| | | *The city's economy thrived thanks to its busy* |
| Mike | person | *After the meeting, everyone turned to* |
| | | *The teacher called on* |
| | | *She handed the report directly to* |
| Trump | person | *The media has been closely following the latest statements from* |
| | | *During the debate, the moderator asked a direct question to* |
| | | *Many supporters gathered outside the venue to catch a glimpse of* |
| expert | person | *After years of practice, she became an* |
| | | *The company hired an* |
| | | *When it comes to antique furniture, he's an* |
| loves | verb | *She truly believes that everyone* |
| | | *The way he looks at her shows how much he* |
| | | *Despite their differences, their friendship* |
| hates | verb | *Everyone knows that she* |
| | | *The way he treats people shows he* |
| | | *It's clear from his expression that he* |
| apple | object | *She reached into the bag and pulled out* |
| | | *The smoothie recipe called for one chopped* |
| | | *He carefully balanced the shiny red* |
| sad | adjective | *After hearing the bad news, she felt incredibly* |
| | | *The movie's ending left everyone feeling* |
| | | *His eyes told a story of being deeply* |
| happy | adjective | *After receiving the good news, she felt extremely* |
| | | *The children were laughing and playing, clearly very* |
| | | *Winning the competition made him incredibly* |

# F  Intervention Test with Feature Direction

## F.1  Generalized Formulation of a Steering-Vector Intervention

Let $x_{1:T} \in \{1, \cdots, V\}^T$ be the input sequence, $E \in \mathbb{R}^{V \times d}$ be the token-embedding matrix, and $\mathcal{G}_1$ to $\mathcal{G}_L$ be the blocks of a decoder-only Transformer. The unperturbed hidden states are

$$H_0 = E[x_{1:T}], \qquad H_\ell = \mathcal{G}_\ell (H_{\ell-1}) \qquad (\ell = 1, \ldots, L).$$

For any layer index $p$, we denote the vectorized activation as

$$A_p = \mathrm{vec}\,(H_p) \in \mathbb{R}^{d \times T}.$$

With different strategies, we extract the steering direction $z_p \in \mathbb{R}^{d \times T}$. For injection at site $s$, we define the linear Jacobian:

$$\Phi_{p \to s} : \mathbb{R}^{d \times T} \to \mathbb{R}^{d_s}$$

obtained by composing linear portions between indices $p$ and $s$. The transported steering direction is

$$z_s = \begin{cases} \Phi_{p \to s} z_p, & \text{if } s > p \\ \Phi_{s \to p}^\dagger z_p, & \text{if } s < p \end{cases}$$

where $\dagger$ denotes the Moore–Penrose pseudo-inverse. When $s = p$, we set $z_s = z_p$. Eventually, we modify the activation at site $s$:

$$\widetilde{A}_s = A_s + \alpha z_s.$$

The network proceeds normally with this perturbation, yielding modified hidden states $\widetilde{H}_\ell$ and logits $\widetilde{y}_{1:T}$.
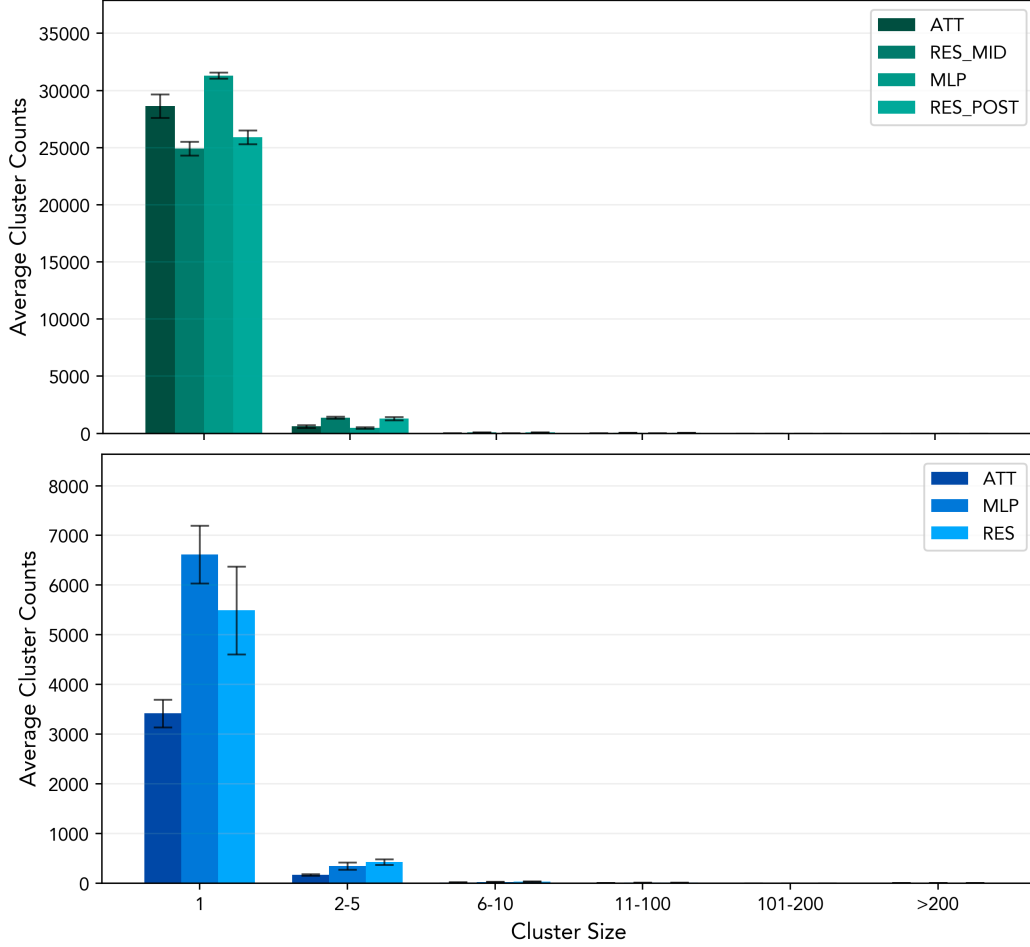
Figure 7: **Interference Cluster Size Distribution**

## F.2 Experiment Details

Our hypothesis posits that if two feature directions interfere in $\mathcal{A}_\ell$, despite being nearly orthogonal in $\mathcal{M}$, then enhancing one will inevitably encode some information of the other one into activation space. If true, this would imply the potential to covertly manipulate the output probability of a target feature by steering the model with seemingly unrelated features. However, we need to point out that multiplying the direction of the interference feature by a scale parameter and adding it to the activation layer within a certain range doesn't always increase the probability of the target feature's top-activating token in the prediction list. Moreover, we also observed that because the interference feature has the highest interference value of 1 with with itself, it also increases the probability of its own top-activating tokens in the output. Sometimes, the output leans more toward the interference feature, which compromises our examination of the impact on the target feature in the top-10 output tokens. Therefore, to focus on studying the influence of semantically different features on the target feature, we separately calculated the similarity between the output and the top-activating tokens of either the target feature or the interference feature in our metrics. If the similarity with the latter exceeds that with the former, it indicates that the semantics are steered toward the interference feature, and we exclude such results from our statistics.

In the specific experiment, we note that features having an interference feature with value above 0.4 constitute only a small proportion. Additionally, high-interference features are mostly semantically similar, which does not align with our research purpose on the mutual influence of different semantics. Therefore, to ensure the richness of high-interference samples in the sampling process, we first select target features from clusters generated based on interference value and then choose interference

18

features for them, also ensuring that the interference features differ both semantically and in terms of top-activating tokens from the target features. Next, we search for other interference features with low interference values to the target features for experimentation. Specifically, other interference features are selected based on the interference values lying in intervals: $[0.0, 0.1]$, $[0.1, 0.2]$, $[0.2, 0.3]$ and $[0.3, 0.4]$. The scale parameter was tested within the range of $[-20, 20]$, and we avoide larger ranges to prevent severe disruption of the model.

Due to limitations on computational power, we sample clusters and features across various layers. In each experiment with `Pythia-70M`, we sample 450 target features and collect approximately 2,000 interference features. In each experiment with `GPT-2-Small`, we sample 1,200 target features and collect approximately 5,000 interference features. As mentioned in the main text, for each feature, we focus on its top-activating token and use `DeepSeek-V3` to generate three prompt sentences for it. For each sentence, we test within the aforementioned scale range and record the result with the greatest improvement in the four metrics. This result means the best performance that the steering vector can achieve to induce the semantic of output toward target feature without significantly disrupting the model. And the final four metrics are averaged across all sentences for all features. To show the robustness of our experiments, more results are listed below.



Figure 8: **Replications of the feature-level intervention on sampled features for** `GPT-2-Small`. Each row is an independent experiment. The target and interference features are all sampled randomly.
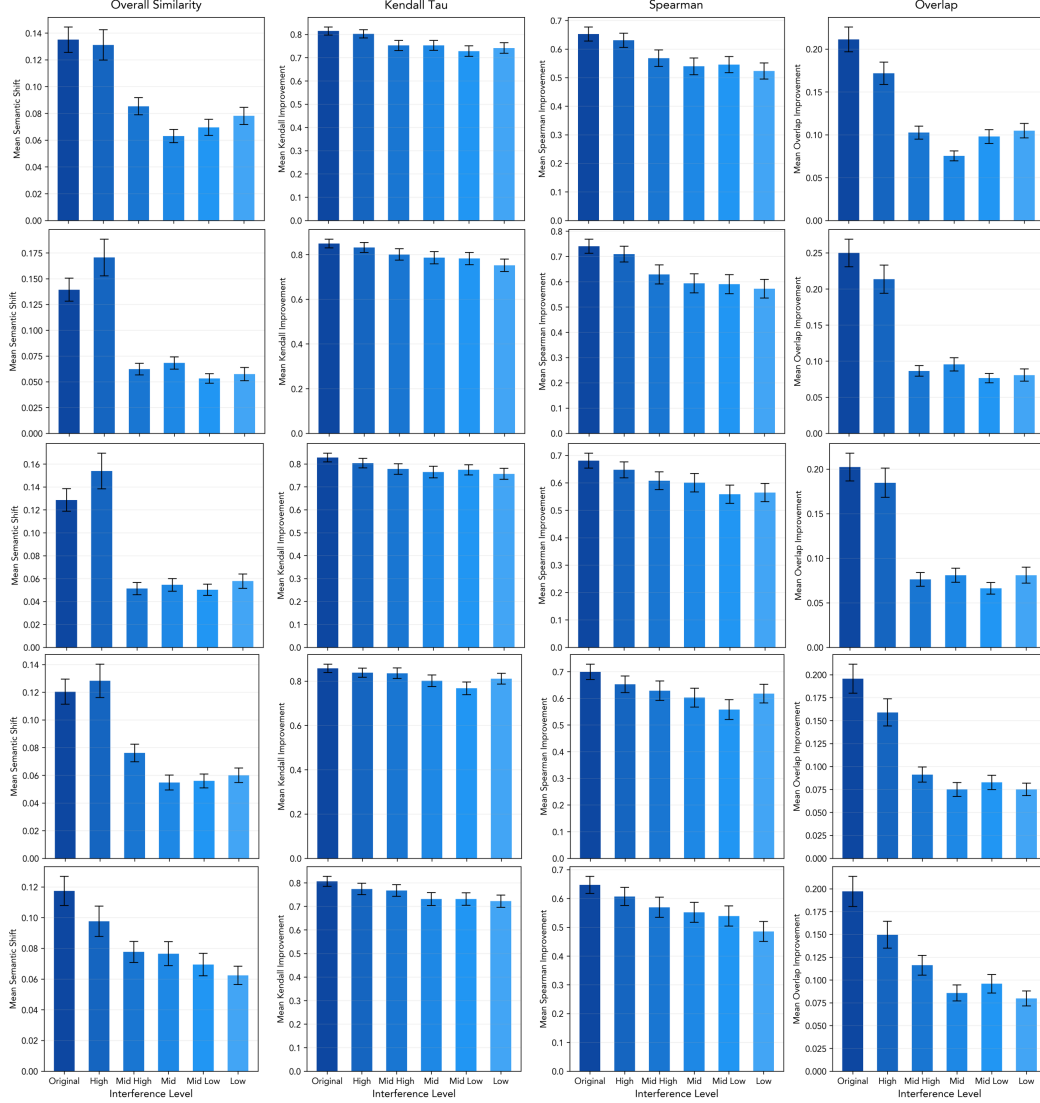
19

Figure 9: **Replications of the feature-level intervention on sampled features for** `Pythia-70M`.
Each row is an independent experiment. The target and interference features are all sampled randomly.

# G   Intervention Test with Token's Gradient

## G.1   Token Gradient Direction Extraction

Given a tokenized input sequence $x = [x_0, \ldots, x_{T-1}]$, let $e_i = E[x_i]$ denote the embedding of token $x_i$, and $\mathbf{e} = [e_0, \ldots, e_{T-1}]$ the full input embedding sequence. Let $f_\ell : \mathbb{R}^{T \times d} \to \mathcal{A}_\ell^T$ denote the model's transformation up to layer $\ell$. The activation at position $i$ is:

$$a_{\ell,i} = f_\ell(\mathbf{e})[i] \in \mathcal{A}_\ell.$$

We define a scalar probe loss that selects this activation via a linear projection vector $v \in \mathbb{R}^d$:

$$\mathcal{L} = \langle a_{\ell,i}, v \rangle.$$

The gradient of this loss with respect to the input embedding $e_i$ is:

$$g_{\ell,i} := \frac{\partial \mathcal{L}}{\partial e_i} = \frac{\partial \langle a_{\ell,i}, v \rangle}{\partial e_i}.$$

We then normalize this vector to obtain a direction in embedding space:

$$\hat{g}_{\ell,i} := \frac{g_{\ell,i}}{\|g_{\ell,i}\|_2}.$$

We refer to $\hat{g}_{\ell,i}$ as the *token gradient direction*—the direction in input embedding space along which perturbations to token $x_i$ most increase its activation in $\mathcal{A}_\ell$ along $v$.

### G.2  Experiment Details

Steering with the feature direction requires a pretrained sparse auto-encoder of the target model, which incorporates substantial computational costs and lacks scalability. To break this limitation, we need to explore a general approach. Observe that the SAE features are activated mainly by the top-activating token in its activation texts, while other tokens are just diluting its expression. Based on this observation, we can obtain a better steering vector by focusing on this particular token, and a sketch is as follows. We first feed the feature's activation text into the model, then compute the gradients of the top-activating token with respect to all neurons in the layer. The resulting gradients are combined to form a vector.

The SAE dataset from *Neuronpedia* contains approximately 50 activation text segments per active SAE feature, each strongly activating its corresponding feature. Due to computational limitations, we try to extract the gradient vectors from the first 3 activation texts of each feature. To enable direct comparison with feature-direction vectors, experiments are conducted on the same target and interference features in the above section. Also we scale the vector within the same range $[-20, 20]$. Additional experimental results are presented below. Each with steering with token gradients combined with steering with feature directions can be done in one hour and a half for `Pythia-70M` and six hours for `GPT-2-Small`, running on a single thread of Intel i7-14700K.

## H  Black-Box Interventions on Larger Models

We hypothesize that the polysemantic structures learned by large language models may exhibit some degree of generalizability. To explore this further, the interference study is extended to larger models without pretrained sparse auto-encoders.

### H.1  Target Selection

We deliberately focus on two feature families—(i) location names and (ii) the polarity antonyms "hate" / "love"—because they satisfy three practical and conceptual criteria that make them ideal first-round probes of polysemantic vulnerabilities.

**High corpus frequency, low internal polysemy.** Most large-scale text corpora mention both world cities/countries and the verbs hate/love thousands of times, giving the SAE a rich activation signal, yet each term carries a relatively unambiguous core meaning. This minimizes confounds from "target drift" when we measure probability shifts.

**Complementary linguistic classes.** Locations are concrete named entities rooted in external knowledge, whereas hate/love are abstract affective predicates that drive sentiment. Showing transferable interference for both a proper-noun category and an emotional-valence category demonstrates that the vulnerability is not restricted to a single part of speech or semantic field.

**Policy relevance.** Manipulating geographic references risks misinformation about real-world facts ("The capital of X is..."), while manipulating strong sentiment verbs directly impacts toxicity and persuasion. Successful steering of these tokens therefore highlights two distinct, societally significant threat surfaces-factual reliability and affective bias.

Together, these criteria make locations and hate/love a parsimonious yet representative pair for an initial, systematic evaluation; expanding to additional categories is an important next step once the core risk is established.

### H.2  Steering with Token Gradient Vector

The scalable intervention on `LLaMA3.1-8B-Instruct` is conducted by first selecting target type tokens as mentioned above and identifying target features in `Pythia-70M` and `GPT-2-Small` for

Figure 10: **Replications of the token-level intervention on sampled features for `GPT-2-Small`.** Each row is an independent experiment. The target and interference features are all sampled randomly.

which these tokens are the top-activating ones. The two interference feature sets in `Pythia-70M` and `GPT-2-Small` with respect to the target features are then identified. Next, we collect the top-activating tokens in two models respectively, and compute the intersection. The figure12 shows a sketch of the shared interference tokens across two models. From the token cloud map, we can observe that high-interference tokens are often punctuation-like tokens such as line breaks. There are also some tokens with specific meanings, which may be related to certain target tokens in daily context.

After getting the tokens, we proceed to collect the activation texts, which may activate interference features of the target in black-box models. Due to computational constraints, we only compute gradients from and perform operations on the first half of residual layers in `LLaMA3.1-8B-Instruct`. The intervention experiments are done for three target token types, each containing about 100 sentences. More intervention examples are listed below. It takes about 20 minutes for a single RTX4090 GPU to find a highly effective gradient vector for steering.
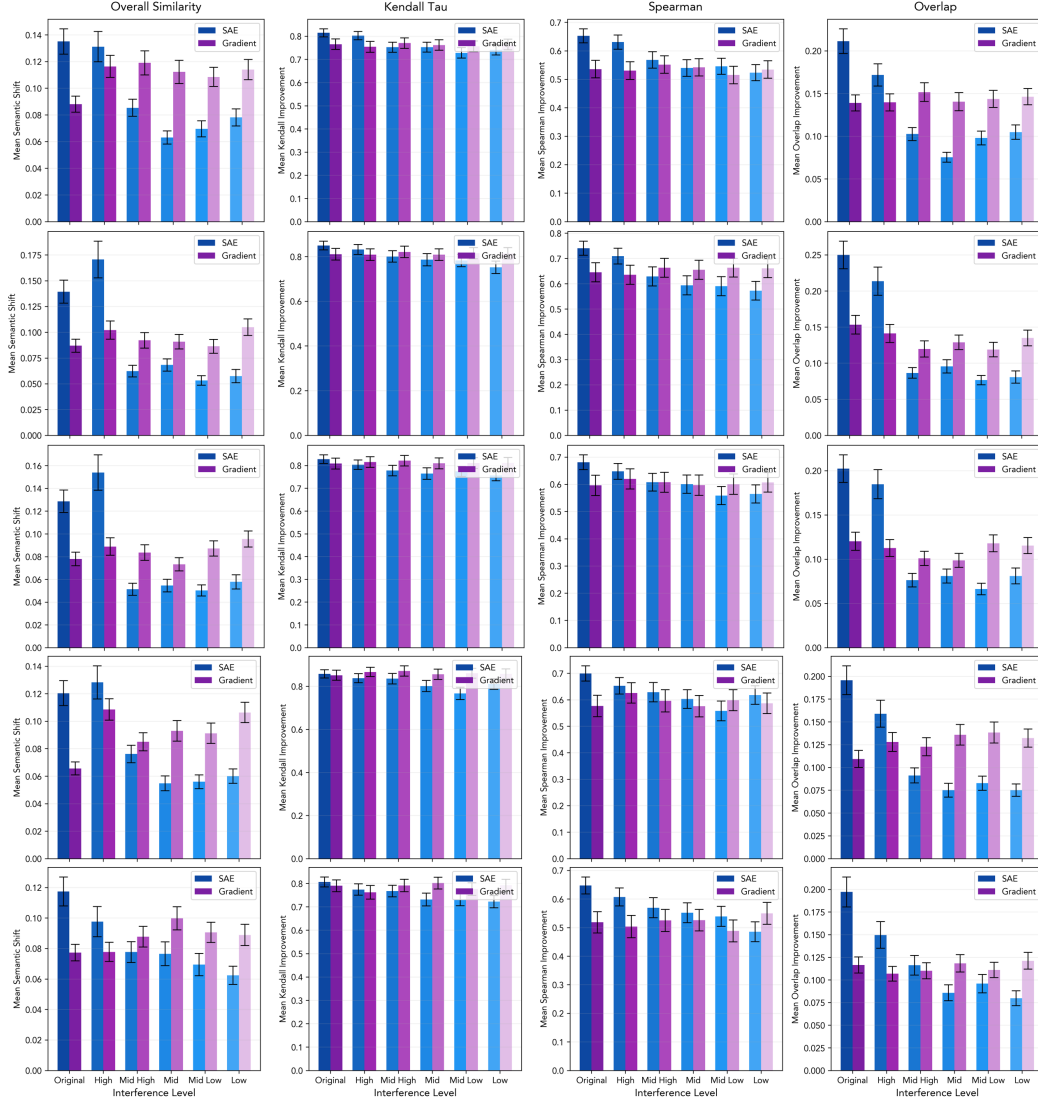
22

Figure 11: **Replications of the token-level intervention on sampled features for** `Pythia-70M`. Each row is an independent experiment. The target and interference features are all sampled randomly.

Table 4: **Examples of interventions on LLaMa3.1-8B-Instruct Using Token Gradient Vector**

| Type | Intervention feature | Result |
|---|---|---|
| location | terms related to data and its presentation | *"After months of planning, our road trip finally reached"* |
| | | ↑ Entered      ↓ Dropped |
| | | New   +0.017    an      -0.006 |
| | | Seattle +0.015    it       -0.007 |
| | | San   +0.011    our     -0.002 |
| | the verb "be" in various forms and contexts | *"She always dreamed of owning a small cafe in"* |
| | | ↑ Entered      ↓ Dropped |
| | | Vienna +0.080   France -0.008 |
| | | Munich +0.071   town   -0.007 |
| | | Berlin   +0.038   Italy    -0.006 |

*Continued on next page*

Table 4 – *Continued from previous page*

| Type | Intervention feature | Result |
|------|----------------------|--------|
| | proper nouns, names, and references to specific roles or positions | *"This novel's opening scene takes place aboard a train to"* <br> ↑ Entered ↓ Dropped <br> Beijing +0.023 New -0.026 <br> Tokyo +0.020 Venice -0.009 <br> Shanghai +0.018 Istanbul -0.010 |
| | quantitative data points related to statistics and performance metrics | *"The rebels established their hidden base deep within"* <br> ↑ Entered ↓ Dropped <br> Afghanistan +0.018 an -0.009 <br> Germany +0.015 their -0.003 <br> Eastern +0.014 one -0.002 |
| | references to specific labeled items or categories | *"His last known coordinates placed him somewhere near"* <br> ↑ Entered ↓ Dropped <br> Paris +0.012 an -0.003 <br> New +0.010 their -0.003 <br> Moscow +0.009 Lake -0.002 |
| name | quantitative data points related to statistics and performance metrics | *"Nobody expected the mysterious package to be from"* <br> ↑ Entered ↓ Dropped <br> Paul +0.261 the -0.104 <br> Emmanuel +0.026 a -0.078 <br> Matthew +0.021 Lake -0.51 |
| | references to academic institutions or concepts | *"The voice on the recording definitely belongs to"* <br> ↑ Entered ↓ Dropped <br> Robert +0.015 a -0.101 <br> Patrick +0.012 the -0.088 <br> David +0.009 me -0.033 |
| | phrases related to pre-approval processes and conditional statements | *"The fingerprints found at the scene match those of"* <br> ↑ Entered ↓ Dropped <br> Michael +0.003 your -0.017 <br> Richard +0.003 one -0.011 <br> Smith +0.004 both -0.008 |
| | keywords related to file management and programming constructs | *"This traditional folk song was popularized by"* <br> ↑ Entered ↓ Dropped <br> Bruce +0.010 Pete -0.086 <br> Walter +0.010 American -0.032 <br> Paul +0.007 Woody -0.021 |
| | terms related to multimedia and video production | *"The confidential information was leaked by former employee"* <br> ↑ Entered ↓ Dropped <br> Mike +0.017 and -0.024 <br> Tom +0.012 who -0.024 <br> Bill +0.011 to -0.010 |
| emotion | instances of the verb "is." | *"After trying the new recipe, my brother absolutely"* <br> ↑ Entered ↓ Dropped <br> love +0.121 fell -0.042 <br> hate +0.095 LO -0.037 <br> dislike +0.015 ad -0.031 |

Table 4 – *Continued from previous page*

| Type | Intervention feature | Result |
|---|---|---|
| | references to legal documents and real estate transactions | *"Science proves that most infants naturally"* <br> ↑ Entered     ↓ Dropped <br> Like +0.048   develop -0.099 <br> like +0.020   prefer -0.051 <br> love -0.001   learn -0.034 |
| | phrases indicating topics of discussion or content focus | *"His body language suggests he secretly"* <br> ↑ Entered     ↓ Dropped <br> love +0.457   wants -0.158 <br> loved +0.012   enjoys -0.069 <br> hate +0.015   hopes -0.062 |
| | phrases indicating relationships and affiliations in contexts such as surveillance, borders, and regulations | *"This fabric texture makes allergy sufferers"* <br> ↑ Entered     ↓ Dropped <br> love +0.126   miserable -0.091 <br> like +0.020   feel -0.074 <br> hate +0.027   and -0.043 |
| | statements that conclude or summarize concepts | *"After the concert critics began to"* <br> ↑ Entered     ↓ Dropped <br> hate +0.017   question -0.070 <br> love +0.016   praise -0.064 <br> enjoy +0.010   dissect -0.054 |

*Note*: ↑ Entered means that corresponding tokens entered the top-10; ↓ Dropped means that corresponding tokens dropped from the top-10. Gray-shaded rows indicate black-box interventions.

## H.3 Prompt Injection

In addition to the success rate of elevating target tokens to top-10 list, we evaluate the injection with other three metics. The first two ones are improvement in weighted cosine similarity and weighted overlap between model's top-10 prediction and target token set. And the third one is improvement in best rank of target tokens in model's top-10 prediction. We collect the best improvement for each sentence. The results of experiments on `Pythia-70M`, `GPT-2-Small`, `LLaMA3.1-8B-Instruct` and `Gemma-2-9B-Instruct` are shown below.13

# I Polysemantic Neuron Manipulation

During the examination of SAE features and their connections with neurons, many features exhibit semantically similar activation texts. To avoid repetitive analysis on similar activation texts, we first perform feature clustering based on semantics of activation texts, and then check neuron connection at the cluster level. Given that the sparse auto-encoder from *Neuronpedia* is trained with a sparsity setting of 3, the analysis focuses on the top three neurons with the highest alignment values per cluster. A threshold of 0.2 is applied to filter out weak connections. Figure15 shows the distribution of polysemantic neurons identified in each layer. We can see that polysemantic neurons with strong connections with aggregated features only take up fewer than 5% in each layer.

For strongly connected polysemantic neurons, we do further investigations on how suppressing or boosting their activation influence the semantic shift in model's output to their aligned features. Neurons' activation is multiplied with a scale value in the range $[0, 20]$. Note that scaling within $[0, 1]$ suppresses activation, while scaling within $[1, 20]$ amplifies it. Results of more repetitive experiments are shown below17.

| (a) Name interference tokens | (b) Location interference tokens | (c) Love/Hate interference tokens |

Figure 12: **Three types of interference tokens**

## J    Ethics Statement, Limitations and Future Works

This study has three key methodological limitations. First, we rely on SAEs to disentangle polyse-
mantic activations; although SAEs are the de-facto tool, their outputs fluctuate with dimensionality
and hyper-parameters, yielding unstable features (Paulo & Belrose, 2025; Heap et al., 2025; Gao
et al., 2024). Second, our interventions steer only one interference feature in one layer, while multi-
feature, cross-layer manipulations could amplify and better obscure the effect (Ameisen et al., 2025).
Third, we quantify vulnerability solely via shifts in immediate next-token probabilities on two small
base models—because only they both expose raw logits and have pre-trained SAEs—then check
coarse transfer on two larger instructed models; establishing how these interventions alter non-trivial
downstream tasks in bigger models is the next stage of this project.

To balance reproducibility with responsible disclosure, we release complete code, evaluation scripts,
and synthetic data, but deliberately omit the matrices that catalogue shared polysemantic directions.
Publishing those mappings would make it easier to weaponize the very vulnerabilities we study,
whereas the available artifacts still permit independent verification of all empirical claims.
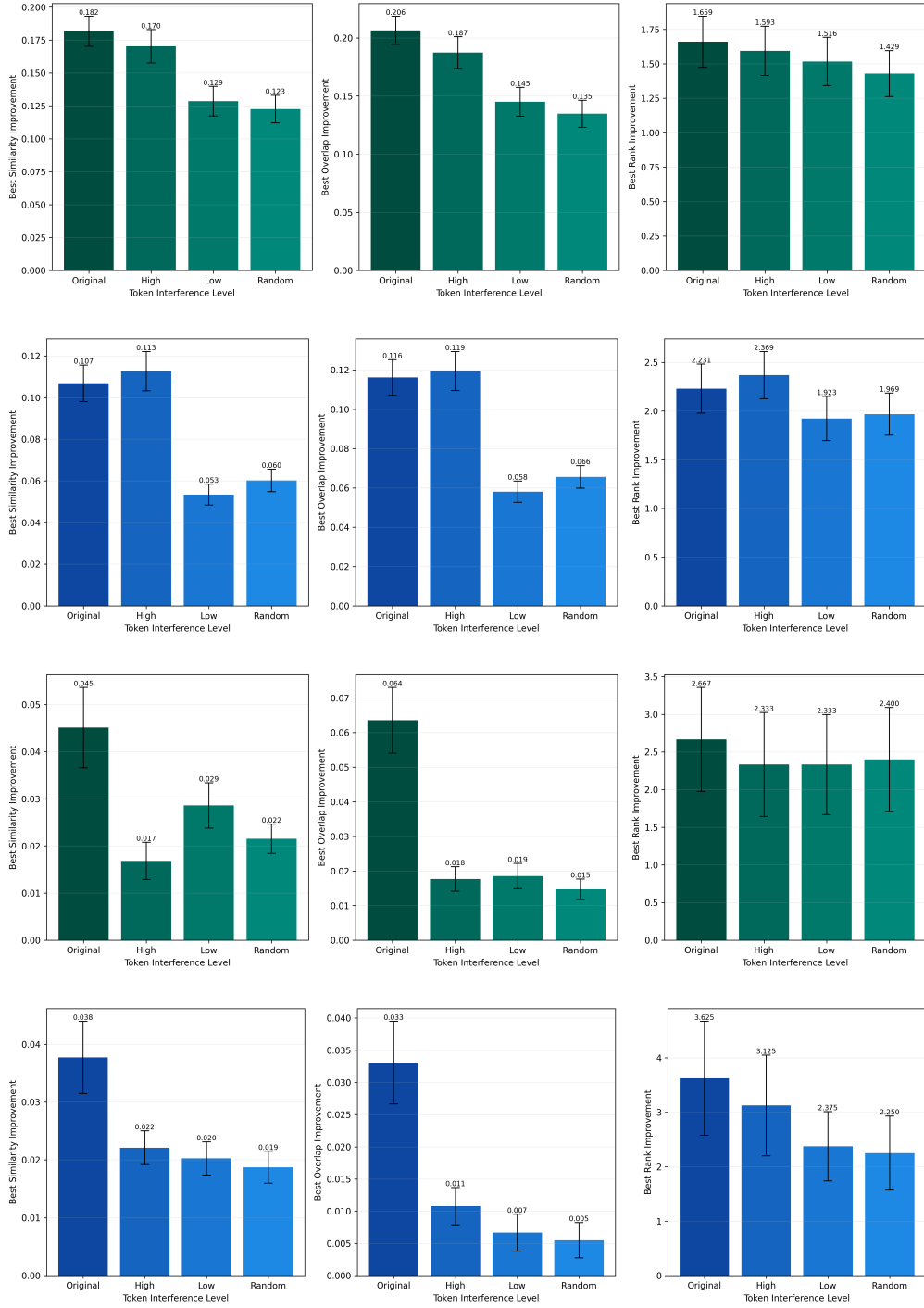
Figure 13: **Three metrics of** `Pythia-70M` **and** `GPT-2-Small` **on location and love&hate token set.** `GPT-2-Small` uses green pillar and `Pythia-70M` uses blue pillar. The above two rows show three metrics evaluated on location type token set. The below two rows show three metrics evaluated on love&hate token set.
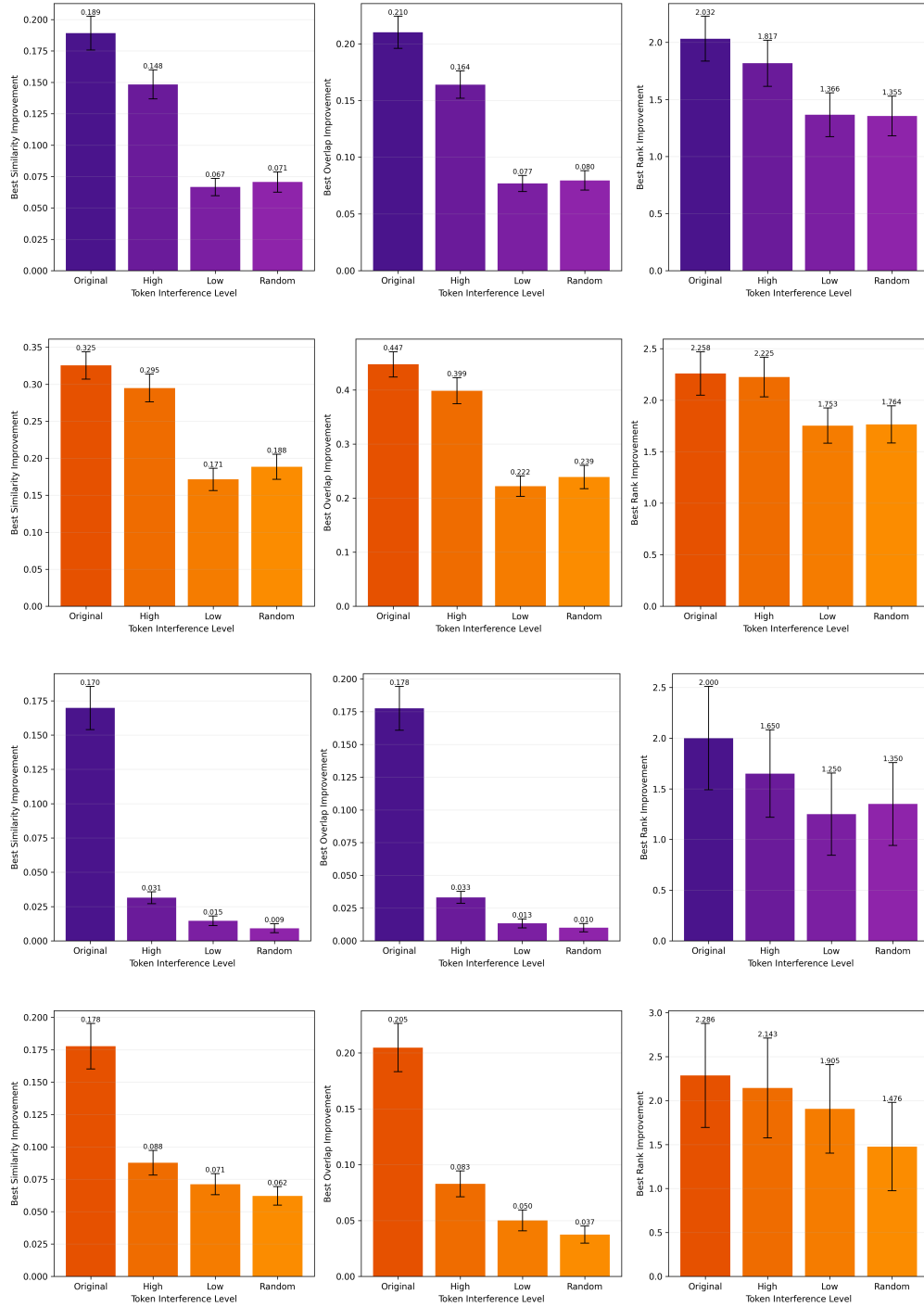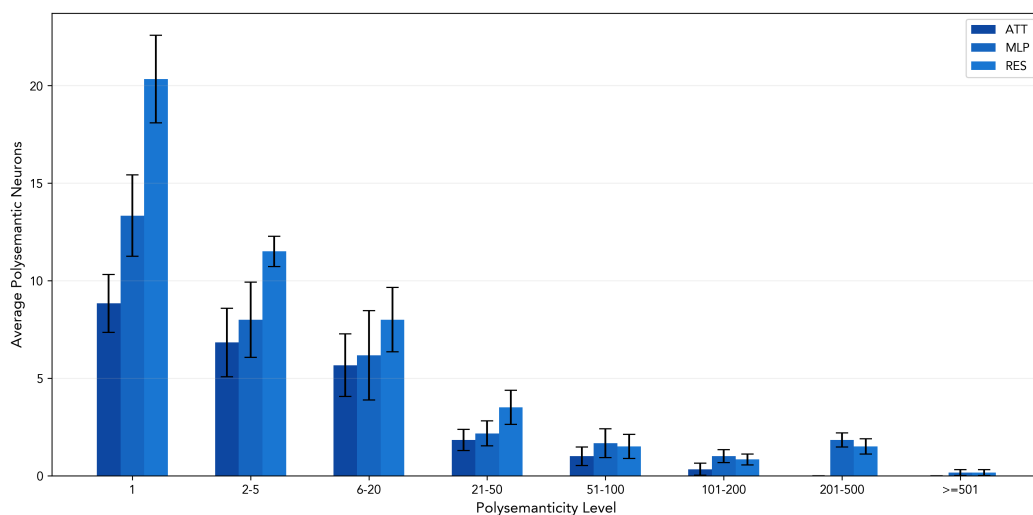
Figure 14: **Three metrics of** `LLaMA3.1-8B-Instruct` **and** `Gemma-2-9B-Instruct` **on location and love&hate token set.** `LLaMA3.1-8B-Instruct` uses purple pillar and `Gemma-2-9B-Instruct` uses orange pillar. The above two rows show three metrics evaluated on location type token set. The below two rows show three metrics evaluated on love&hate token set.

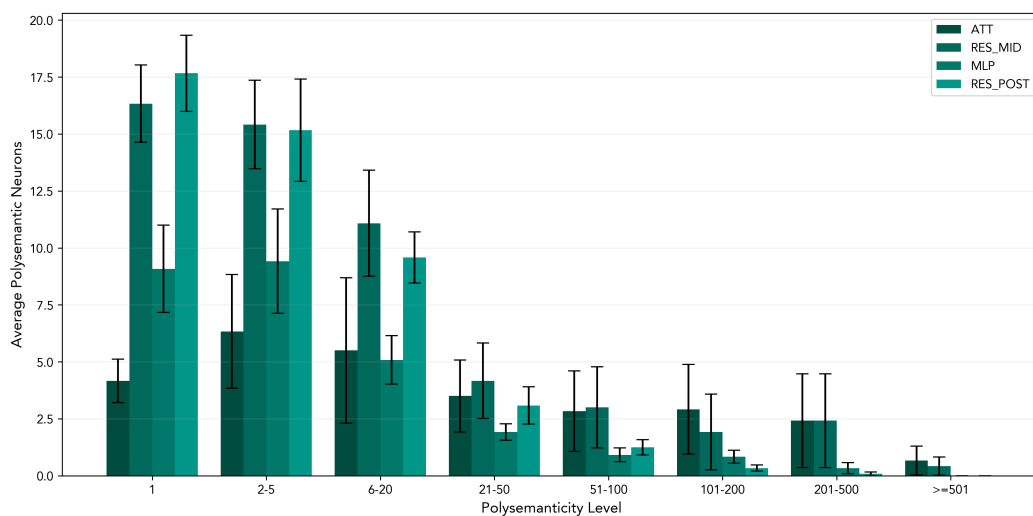Figure 15: **Distribution of polysemantic neurons in** `Pythia-70M`.



Figure 16: **Distribution of polysemantic neurons in** `GPT-2-Small`.
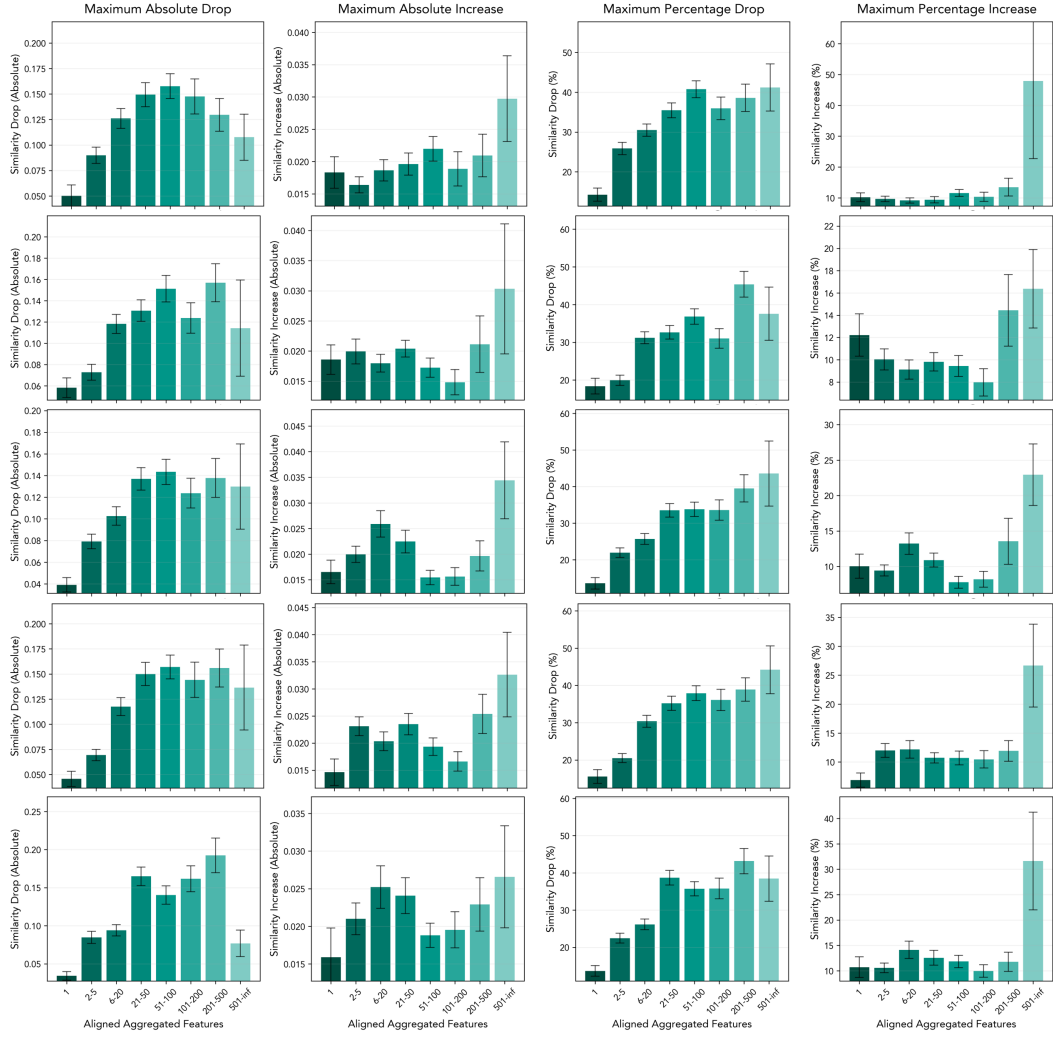
Figure 17: **Replications of the neuron-level intervention on sampled neurons for GPT-2-Small.**
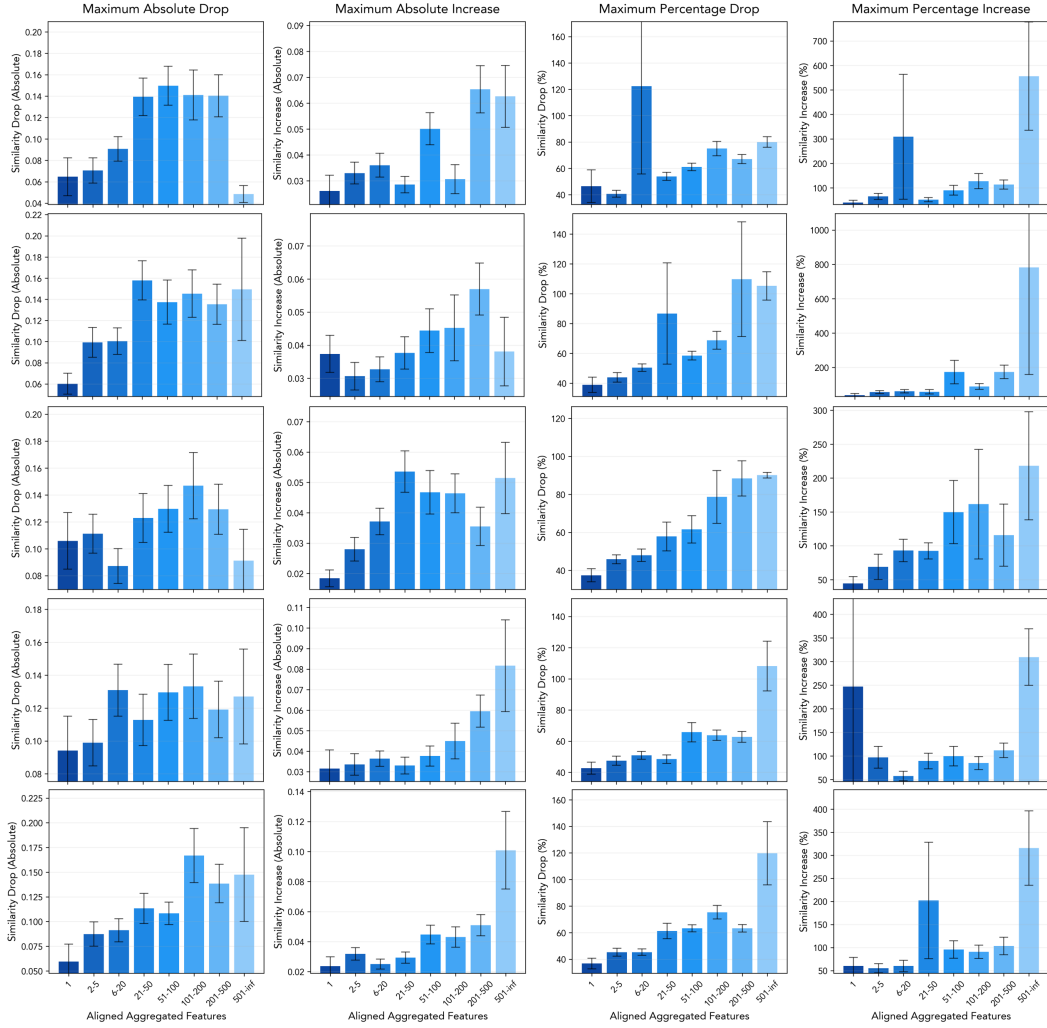
Figure 18: **Replications of the neuron-level intervention on sampled neurons for Pythia-70M.**